ICSV14
Cairns • Australia
9-12 July, 2007

14th International Congress on Sound & Vibration

AN ASSESSMENT OF ALTERNATIVE SENSOR TECHNOLOGY FOR TRANSFER MATRIX MEASUREMENTS IN COMBUSTORS

Jonas P. Moeck, Holger J. Konle, Christian Oliver Paschereit

Institut für Strömungsmechanik und Technische Akustik
Technische Universität Berlin
10623 Berlin, Germany

jonas.moeck@pi.tu-berlin.de

Abstract

Acoustic transfer matrices are an important modeling tool for muffler design and thermoacoustic system analysis. They allow for a relatively simple and modular description of (thermo-) acoustic systems in which only plane waves propagate. However, in case of combustion systems, where the flame transfer matrix (or the scalar flame transfer function) is one of the most important modeling inputs, measuring conditions are quite harsh due to high temperatures (well above 1000 °C) and possibly high static pressures. The applicability of two high-temperature resistant pressure sensors to transfer matrix measurements is, therefore, assessed in this work. The first is a probe microphone designed according to the semi-infinite coil principle. As a second alternative, a fiber optic microphone is considered. This less common pressure sensor is built from a thin metallic membrane and a vibrometer detecting the transversal displacement. Two acoustic elements are considered, a uniform duct and a circular orifice. The transfer matrices obtained using the two alternative sensors are compared to measurements with wall flush-mounted standard 1/4" condenser microphones. The results show reasonable agreement and demonstrate the general applicability of the alternative sensors to transfer matrix measurements.

1. INTRODUCTION

Acoustic transfer matrices are a useful concept in various areas of application. Modeling of mufflers [1] and thermoacoustic systems [2] are only two examples were extensive use is made of this approach. The advantage lies in a very simple acoustic representation of an element where, at the inlet and at the outlet, only plane waves propagate. In addition to that, it is relatively easy to connect several elements and obtain the acoustic response for a combined system or model a lumped boundary condition of a more complex geometrical set up. Even flow-acoustic and flow-combustion-acoustic interactions in the linear regime can be modeled using this approach (see, e.g., Hofmans et al. [3] and Schuermans et al. [4]). However, if transfer matrices contain information about elements with flow or combustion, analytical or numerical access might be very limited. In these cases, experimental methods have to be used.

In the last two decades, the so called Multi-Microphone-Technique (MMM) [4–6] has been proven to be the state of the art for this task. The usual experimental procedure is to use several condenser microphones (either 1/4" or 1/2") to assess the acoustic pressure at several axial locations. This is necessary to find the four scalar complex valued functions of frequency that constitute the transfer matrix. In case of combustion systems, for which the flame transfer matrix (or the scalar flame transfer function) is one of the most important modeling inputs [7, 8], measuring conditions are quite harsh due to very high temperatures (up to 1600 °C) and possibly high static pressures. Flame transfer matrix measurements are therefore accomplished using water-cooled microphone holders [4, 5, 7]. These are difficult to design with no impact on the pressure frequency response and still cannot fully protect the microphone against harsh combustor conditions. Also, a condenser microphone is very sensible to electromagnetic interference.

For these reasons, two alternative methods to assess the pressure under harsh conditions for transfer matrix characterization are investigated here. The first makes use of a probe holder built upon the semi-infinite coil principle. In this approach, the actual pressure sensor is remotely located outside the combustor, and the pressure is guided through a thin tube. Such devices were built by several researchers for dynamic pressure measurements in combustors [9–11]. To our knowledge, however, none of them tried to apply this type of sensor to transfer matrix measurements. One potential problem is that the frequency response of these probe microphones with respect to the wall pressure is always affected by the remoting system. The second sensor is a fiber optic microphone, a combination of a laser vibrometer and a high temperature resistant reflecting diaphragm.

2. HIGH-TEMPERATURE RESISTANT PRESSURE SENSORS

2.1. Fiber optic microphone

The fiber optic microphone (FOM) used in this study is still under development, but to evaluate its current status with respect to applications, transfer matrix measurements were conducted. A reflecting membrane, a glass fiber, and an interferometer are the main components of the FOM. The vibrometer (glass fiber and interferometer) detects surface displacement by means of laser beam interference. The spatial separation of membrane and transducer electronics makes this sensor uniquely adequate for the application to pressure measurements in high temperature or even EMI (Electro Magnetic Interference) or RFI (Radio Frequency Interference) environments. In the frequency range considered here, the FOM exhibits a noisy but approximately flat frequency response with respect to a wall flush-mounted condenser microphone (see Fig. 2). Also, it can be noted, that the FOM delivers the unsteady pressure with no delay, which makes it particularly attractive as a sensor for control applications. More details on the FOM, including the dependence of the acoustic response on design parameters as, e.g., border tension, as well as the linearity of the response were presented by Konle et al. [12].

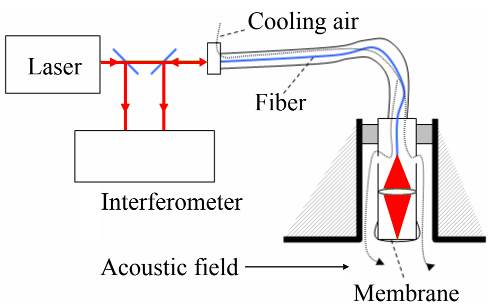

Figure 1. Fiber optic microphone principal set-up

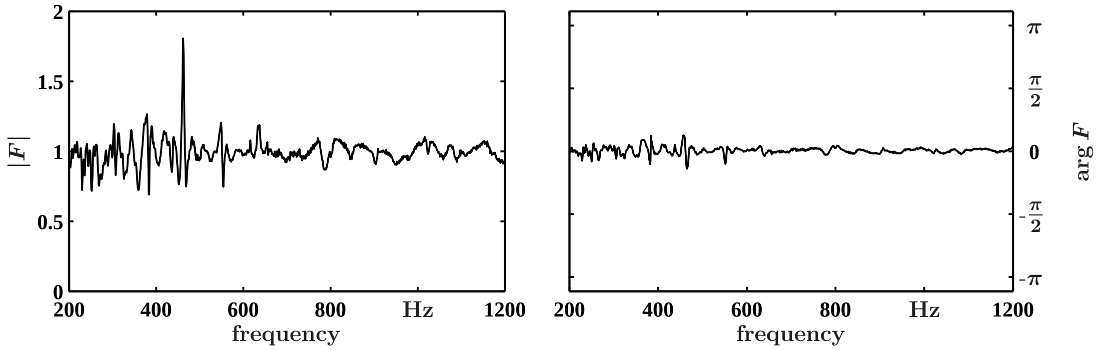

Figure 2. FOM transfer function with respect to wall flush-mounted microphone

2.2. Probe microphone

The probe holder considered in this work was designed and manufactured by the German Aerospace Center, Institute of Propulsion Technology, Berlin, and has been used in a number of combustion instability characterization and control investigations (see, e.g., Bake et al. [13] or Moeck et al. [14]). Figure 3 displays the design of the probe holder. The microphone is acoustically connected to the measurement location via a steel tube (2 mm diameter). To avoid resonances in the connecting duct, the microphone is mounted perdendicularly to the tube, and the tube is elongated to approximately 1 m. In this way, visco-thermal effects significantly attenuate the acoustic waves and, thereby, minimize reflections from the tube end. Due to this set up, the response of the microphone in the probe assembly will be different compared to a measurement with a wall flush-mounted microphone. The transfer function of the probe microphone with respect to a flush-mounted sensor is displayed in Fig. 4. The results for three different probe holders are presented, showing virtually no difference in the response up to 1 kHz. In addition to the experimental data, the transfer function of a transmission line model of the probe microphone is also added. A straightforward plane wave calculation shows that the transfer function of the probe holder can be written as

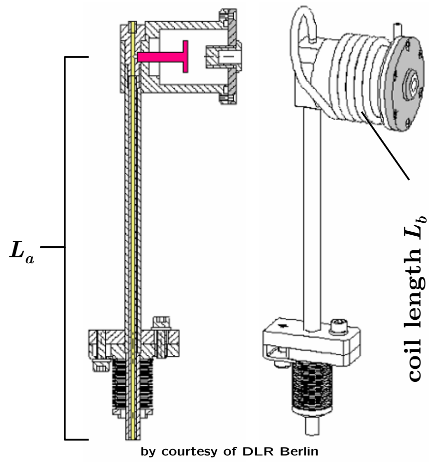

Figure 3. Probe microphone design

$$F = \frac{p_1}{p_0} = \frac{e^{L_a k\Gamma}\left(e^{2L_b k\Gamma} + R\right)}{e^{2(L_a+L_b)k\Gamma} + R}, \tag{1}$$

where k denotes the wave number of the plane mode, L_a is the distance between measurement location and microphone, L_b is the coil length, R the reflection coefficient at the end of the coil (which has been assumed to be -1), and p_0 and p_1 denote wall pressure and pressure in the transmission line at the microphone position, respectively. Γ represents the complex (frequency dependent) propagation constant taking into account visco-thermal damping. Here, Γ has been calculated from the low reduced frequency approximation of the full Kirchhoff solution (see, e.g., Tijdeman [15]). The oscillatory behavior of the transfer function (Fig. 4) is due to wave reflections at the end of the coil, which are not damped completely. As a result of the spatial

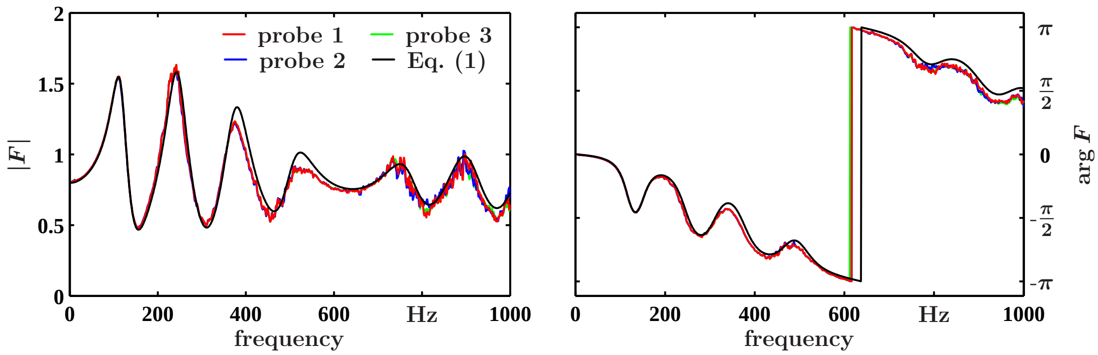

Figure 4. Probe microphone transfer function; model and experimental data

separation of measurement location and microphone position, there is a time delay of L_a/c (c denoting speed of sound) in the probe response with respect to a wall flush-mounted microphone, corresponding to the negative slope of the linear decrease in the phase response (Fig. 4). There is good agreement of the modeled transfer function of the probe holder (Eq. (1)) and the experimental data. Detailed information on the probe microphone was presented by Forster et al. [16], as, e.g., the influence of a purge flow in the coil on the frequency response.

3. TRANSFER MATRIX MEASUREMENTS

The acoustic transfer matrix is defined as a 2×2 mapping of acoustic variables representing the plane wave mode. This mapping provides frequency response information about a certain acoustic element. Strictly speaking, the transfer matrix maps acoustic pressure p and axial particle velocity u at the upstream location of the element to pressure and velocity at the downstream location. This can be written as

$$\begin{bmatrix} p_d \\ u_d \end{bmatrix} = \begin{bmatrix} T_{11} & T_{12} \\ T_{21} & T_{22} \end{bmatrix} \begin{bmatrix} p_u \\ u_u \end{bmatrix}, \tag{2}$$

where subscripts u and d denote up- and downstream locations, respectively. Here, as in the following, the acoustic pressure is assumed to be scaled by the characteristic impedance ρc, ρ being the fluid density. The elements of the transfer matrix are complex valued functions of frequency. An equivalent description is given by the scattering matrix, which defines a mapping between the Riemann invariants. The Riemann invariants are, simply speaking, the wave amplitudes of the up- and downstream traveling waves. The relation to the primitive acoustic variables is given by

$$\frac{p}{\rho c} = f + g, \qquad u = f - g, \tag{3}$$

where f and g represent down- and upstream traveling waves, respectively. Accordingly, the scattering matrix **S** maps the incident waves to the outgoing, viz.,

$$\begin{bmatrix} f_d \\ g_u \end{bmatrix} = \begin{bmatrix} S_{11} & S_{12} \\ S_{21} & S_{22} \end{bmatrix} \begin{bmatrix} f_u \\ g_d \end{bmatrix}. \tag{4}$$

To determine the four transfer (or scattering) matrix elements, at least two independent acoustic states are required. One way to generate the two states is to excite the acoustic field at up- and downstream locations. Acoustic pressure and velocity or, equivalently, the Riemann invariants can be determined from pressure measurements at multiple (at least two) axial locations. This is called the Multi-Microphone-Method (MMM) [4, 17]. Using only microphones to determine the plane wave acoustic field has the advantage that no velocity probe is necessary. Measuring the acoustic particle velocity (usually associated with very small amplitudes) directly is difficult and, therefore, error prone.

In a duct of constant cross-section, the frequency domain plane wave acoustic field in a quiescent fluid can be written as [1]

$$p(x,\omega) = f(\omega)\exp(-\mathrm{i}kx) + g(\omega)\exp(\mathrm{i}kx), \tag{5a}$$

$$u(x,\omega) = f(\omega)\exp(-\mathrm{i}kx) - g(\omega)\exp(\mathrm{i}kx), \tag{5b}$$

where $k = \omega/c$ is the wave number of the plane wave field (neglecting visco-thermal damping) and $\mathrm{i} = \sqrt{-1}$. Given the experimentally determined pressure phasors at multiple axial locations, Eq. (5) can be formally inverted in a least squares sense to yield

$$\begin{bmatrix} f(\omega) \\ g(\omega) \end{bmatrix} = \mathbf{Z}^{+} \begin{bmatrix} p(x_1,\omega) \\ p(x_2,\omega) \\ \vdots \\ p(x_n,\omega) \end{bmatrix}, \quad \text{with} \quad \mathbf{Z} = \begin{bmatrix} \exp(-\mathrm{i}kx_1) & \exp(\mathrm{i}kx_1) \\ \exp(-\mathrm{i}kx_2) & \exp(\mathrm{i}kx_2) \\ \vdots & \vdots \\ \exp(-\mathrm{i}kx_n) & \exp(\mathrm{i}kx_n) \end{bmatrix}, \tag{6}$$

and $(\cdot)^{+}$ denotes the pseudoinverse. Once f and g are known, the plane wave pressure field in a duct of constant cross-section is completely determined, and p and u at an arbitrary location (in that duct) can be calculated.

Given now complex wave amplitudes up- and downstream of the element for two different acoustic states, the scattering matrix can be calculated from

$$\mathbf{S} = \begin{bmatrix} f_d^A & f_d^B \\ g_u^A & g_u^B \end{bmatrix} \begin{bmatrix} f_u^A & f_u^B \\ g_d^A & g_d^B \end{bmatrix}^{-1}, \tag{7}$$

where superscripts A and B correspond to the two independent excitation states. In view of Eq. (3), the transfer matrix can be computed in a similar way.

3.1. Transfer matrix measurements using wall flush-mounted condenser microphones

In standard transfer matrix measurements for muffler or flame characterization in the linear regime, several 1/4" microphones are used simultaneously to assess the acoustic pressure at different axial positions, flush-mounted to the channel wall. To determine frequency domain phasors, the data is usually correlated with the excitation signal and averaged to suppress random noise contributions [6]. A proper calibration for the microphones is necessary to identify the plane wave field. This can be either a one-point-calibration using a pistonphone at one frequency or a relative calibration, where all microphones are exposed to the same acoustic field and all Fourier spectra are referenced to one baseline microphone. In the latter case, frequency dependent calibration coefficients are obtained, that include magnitude and phase information.

The latter method is more accurate, in particular in the low frequency regime, and allows to reliably detect faulty sensors.

Two typical excitation and signal processing techniques are frequency sweeps and stepped sine in combination with cross-spectrum based frequency domain averaging. However, various alternative possibilities exist (see, e.g., Allam & Bodén [6] and references therein). Since the experiments where conducted in an environment with a low noise level, sweep excitation was used. Note, however, that in combustors with high thermal power, stepped sine excitation is the only way to obtain reasonable results.

3.2. Transfer matrix measurements using FOM and probe microphone

Since only one FOM prototype was available, the acoustic pressure for one excitation state could not be acquired simultaneously at different axial positions. For this reason, the same FOM was mounted to the channel at three different locations successively, on the up- and downstream side, and was exposed to the same acoustic field at each position, corresponding to the two independent excitation states. To allow for a meaningful comparison, the same procedure was used for the probe microphone. The axial locations for the sensor mountings were the same as in the case of measurements using condenser microphones. Using only one sensor for all measurement locations, it was not necessary to take into account the frequency response of the FOM and the probe microphone (i.e., a calibration) with respect to a wall flush-mounted condenser microphone since this cancels out in the transfer matrix computation.

4. EXPERIMENTAL SET-UP

The experiments were conducted in the acoustic test facility shown in Fig. 5. Up to 80 microphones in total can be mounted at ten different axial and eight different azimuthal positions. However, since in this study plane wave properties were studied, only one azimuthal position was used. Also, only three axial positions each, up- and downstream of the acoustic element, were equipped with microphones. The axial measurement positions and the location of the acoustic element are shown in Fig. 5. The duct is made of aluminum with a wall thickness of 10 mm and has a diameter of 140 mm. Accordingly, the cut-on frequency for the first non-planar mode is at $f_{10} = 1435$ Hz at ambient conditions [1]. The up- and downstream ends of the test rig are equipped with anechoic terminations.

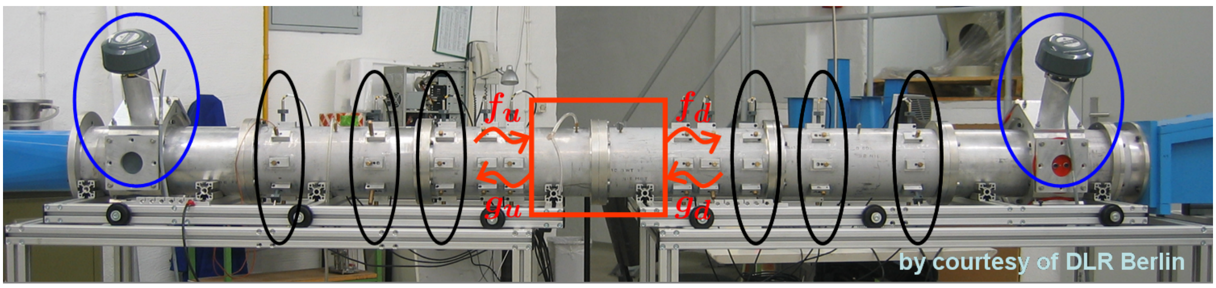

Figure 5. Experimental set up; speakers for acoustic excitation (marked blue), axial measurement positions (marked black) and acoustic element for transfer/scattering matrix determination (marked red)

5. RESULTS AND DISCUSSION

Two generic acoustic elements were considered in this study, a uniform duct of length 400 mm and a circular orifice with inner diameter 40 mm and thickness 3 mm. In case of the uniform duct, the scattering matrix is considered since it has a remarkably easy representation. The acoustic waves travel through the element without reflection. Only the phase is changed due to the propagation time, which is given by $\tau = L/c$, where L is the duct length. Therefore, the scattering matrix for a uniform duct simply reads

$$\mathbf{S}_{\text{duct}} = \begin{bmatrix} e^{-\mathrm{i}\omega\tau} & 0 \\ 0 & e^{-\mathrm{i}\omega\tau} \end{bmatrix} . \tag{8}$$

Due to lack of space, not the full scattering and transfer matrices will be presented but only one representative element. Figure 6 shows the measured upper left scattering matrix element for the uniform duct (left column). There is perfect agreement with the theoretical result (Eq. (8)) in case of the wall flush-mounted microphones (top left). The only deviation that can be observed appears close to 1400 Hz. This can be attributed to higher, non-planar modes, which are excited by the laterally mounted speakers and decay at a slow rate in axial direction close to the cut-on frequency.

The S_{11} element as obtained from measurements using the FOM is shown in the middle left frame of Fig. 6. The results are markedly not as good as in the case of condenser microphone measurements. The magnitude is about 10 % too small, but the slope of the phase is accurately captured. Also, the data scatter is slightly higher. Altogether, there is still reasonable agreement

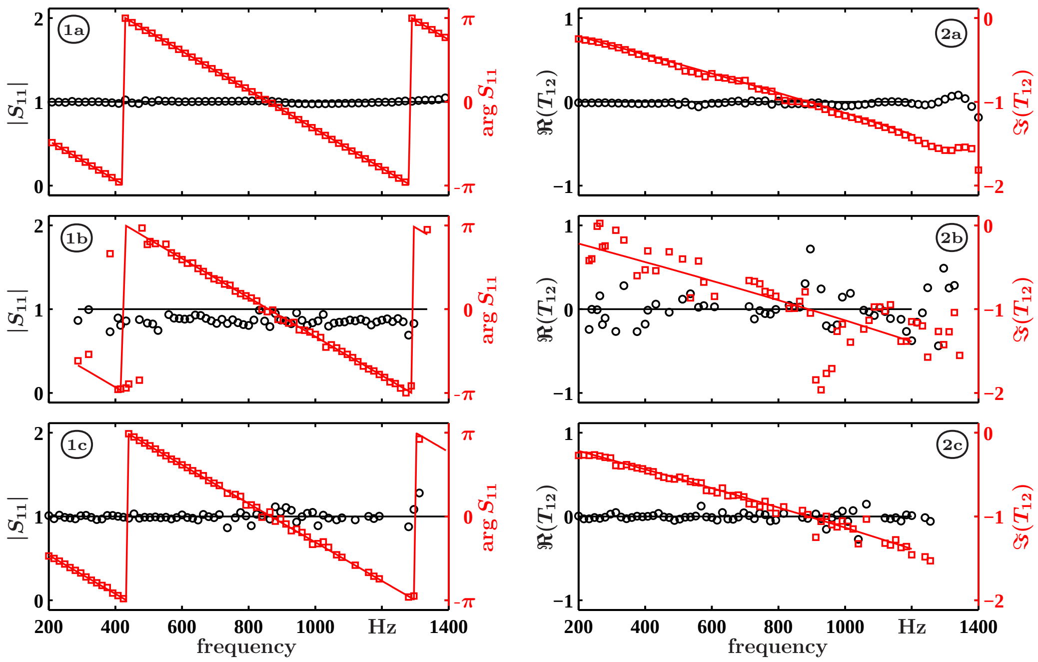

Figure 6. Left column: S_{11}-element of the duct scattering matrix. Right column: T_{12}-element of the orifice transfer matrix. Top row: wall flush-mounted microphones. Middle row: FOM. Bottom row: probe microphone. Solid lines correspond to the theoretical result (Eq. (8)) in case of the duct and to the finite element calculation in case of the orifice. Symbols represent measured data

with the theoretical solution. The results from the probe microphone are more accurate (bottom left in Fig. 6). Magnitude and phase of S_{11} are properly represented. A higher data scatter compared to the measurements with wall flush-mounted microphones (Fig. 6, top left) is apparent, though, in particular between 800 and 1000 Hz.

The results for the T_{12}-element of the transfer matrix of the circular orifice are presented in the right column of Fig. 6. For comparison, T_{12} as obtained from a finite element computation based on the Helmholtz equation (see, e.g., Peat [18]) is also shown. Note that this is in perfect agreement with the so-called $L - \zeta$ model [5] for an acoustically compact element, which, in case of equal cross-sections up- and downstream of the element and with no mean flow, is given by $T_{12} = -\mathrm{i}kL_{\mathrm{eff}}$. Again, the results from the condenser microphone measurements agree quite well with those from the finite element solution. The transfer matrix element obtained with the FOM is significantly more scattered. The general trend of real and imaginary parts can be recognized but the results are certainly not sufficiently accurate to apply this sensor to the determination of unknown transfer matrices. In contrast, the T_{12} element of the orifice is well obtained from the measurements with the probe microphone. The results are not as good as those from the wall flush-mounted pressure sensors, but the real and imaginary part clearly agree with the FEM solution. In case of the FOM and the probe microphone measurements, a coherence filter was applied to the measured scattering and transfer matrices. Only the results at those frequencies were plotted, where the coherence of all sensor signals (at the six axial locations) with respect to the excitation command was close to unity.

The crucial point in the determination of the scattering (or transfer) matrix is the identification of the f and g waves from the complex pressure amplitudes at the axial measurement locations. As a quality indicator of this identification process, the normalized *wave identification residual* (WIR) δ is defined as

$$\delta = \frac{||\left(\mathbf{I} - \mathbf{Z}\mathbf{Z}^{+}\right)\mathbf{p}||}{||\mathbf{p}||}, \tag{9}$$

where $\mathbf{Z}$ is given in Eq. (6) and $\mathbf{p}$ is a vector containing the complex pressure amplitudes corresponding to one excitation state and one microphone group (either up- or downstream of the element). $\mathbf{I}$ is the identity matrix of dimension n (in this case $n = 3$) and $||\cdot||$ denotes the l^2-norm. For $n > 2$ and incommensurate microphone spacings, δ can only vanish if there exist complex values of f and g, such that Eq. (5a) is satisfied for all complex pressure amplitudes in one group. δ maps to values in $[0, 1]$, where low values indicate a good wave identification process.

The WIR for the duct scattering matrix measurements with condenser microphones, FOM, and probe microphone is displayed in Fig. 7. The four curves in one plot correspond to the two excitation states, each with two microphone groups, up- and downstream of the element, respectively. For the condenser microphone measurements, the WIR has values of a few percent up to 1200 Hz, indicating an accurate wave identification process. Larger values of δ for frequencies greater than 1200 Hz can again be attributed to the first circumferential mode. The WIR for the FOM measurements has much larger values over the whole frequency range considered. This means that the wave identification process has a much lower quality compared to the condenser microphone measurements and is consistent with the data scatter in Fig. 6 (middle row). In case of the probe microphone measurements, the WIR is significantly lower, indicating a more accurate identification of the f and g waves from the measured pressure phasors. The highest

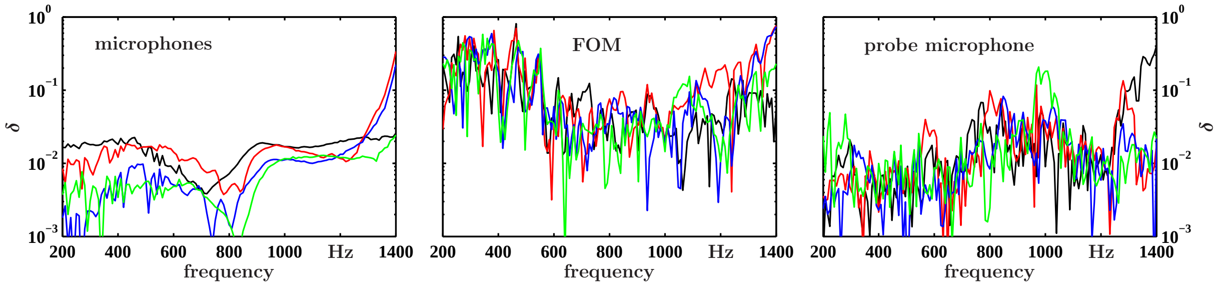

Figure 7. Wave identification residual for measurements with condenser microphones (left), FOM (middle) and probe microphone (right). Different lines correspond to the microphone groups for the two excitation states, up- and downstream of the element, respectively

values are attained at frequencies between 800 and 1000 Hz (disregarding the increase close to the cut-on frequency for the first circumferential mode). This coincides with the frequency range where the data scatter in S_{11} is largest (see left middle frame in Fig. 6). Also, it can be noted that the probe microphone transfer function (Fig. 4) is somewhat contaminated with noise in this frequency regime.

As stated in Sec. 3.2, when using only one sensor at different axial measurement locations, the transfer function with respect to the wall pressure cancels out when computing the scattering or transfer matrix. Therefore, this cannot be a source of the high data scatter in the results from the FOM measurements. Errors might have been introduced through the mounting and demounting of the sensor at the different axial locations. On the other hand, the same procedure was used for the probe microphone, where clearly more accurate results were obtained. A source of errors could be a not fully linear response of the FOM (see Konle et al. [12]).

6. CONCLUSIONS

The principal applicability of two high-temperature resistant pressure sensors, a fiber optic microphone and a probe microphone, to transfer matrix measurements was studied. Two generic acoustic elements were considered, a uniform hard-walled duct and a circular orifice. Reasonable results were obtained with both sensors. In case of the probe microphone, the measured transfer matrices were only slightly less accurate than those obtained from conventional wall flush-mounted pressure sensors. Although the fiber optic microphone showed satisfactory results for the straight duct, high data scatter contaminated the transfer matrix in case of the orifice.

The results presented indicate that the probe microphone can be used to measure transfer matrices in high-temperature environments. However, in the presence of flow and combustion, there is a much higher noise level than considered in this study. The fiber optic microphone clearly needs further improvement before it can be utilized for accurate measurements in this application.

ACKNOWLEDGEMENTS

We kindly thank the combustion group of the German Aerospace Center, Berlin, for making the probe microphones available to us. Financial support from the German Science Foundation through the Collaborative Research Center 557 “Control of Complex Turbulent Shear Flows” as well as from the Helmholtz Association as part of the Young Investigators Group "New Optical Measurement Techniques for Turbomachinery Diagnostics" is gratefully acknowledged.

REFERENCES

[1] MUNJAL, M. L., 1987. *Acoustics of Ducts and Mufflers*. Wiley & Sons, Inc.

[2] LIEUWEN, T. C., AND YANG, V., eds., 2005. *Combustion Instabilities in Gas Turbine Engines*, Vol. 210 of *Progress in Astronautics and Aeronautics*. AIAA, Inc.

[3] HOFMANS, G. C. J., BOOT, R. J. J., DURRIEU, P. P. J. M., AND AURÉGAN, A., 2001. "Aeroacoustic response of a slit-shaped diaphragm in a pipe at low Helmholtz number, 1: Quasi-steady results". *J. Sound Vib.,* **244**(1), pp. 35–56.

[4] SCHUERMANS, B., BELLUCCI, V., GUETHE, F., MEILI, F., FLOHR, P., AND PASCHEREIT, C. O., 2004. "A detailed analysis of thermoacoustic interaction mechanisms in a turbulent premixed flame". ASME Paper 2004-GT-53831.

[5] SCHUERMANS, B., POLIFKE, W., AND PASCHEREIT, C. O., 1999. "Modeling of transfer matrices of premixed flames and comparison with experimental results". ASME Paper 1999-GT-0132.

[6] ALLAM, S., AND BODÉN, H., 2005. "Methods for accurate determination of acoustic two-port data in flow ducts". In *Proc. 12th Intl. Congr. Sound Vib.*, Lisbon, Portugal.

[7] SCHUERMANS, B., BELLUCCI, V., AND FLOHR, P., 2004. "Thermoacoustic flame transfer function of a gas turbine burner in premix and pre- premix combustion". AIAA Paper 2004-0456.

[8] CHEUNG, W. S., SIMS, G. J. M., COPPLESTONE, R. W., TILSTON, J. R., WILSON, C. W., STOW, S. R., AND DOWLING, A. P., 2003. "Measurement and analysis of flame transfer function in a sector combustor under high pressure conditions". ASME Paper GT2003-38219.

[9] STUTTAFORD, P. J., MARTLING, V., GREEN, A., AND LIEUWEN, T. C., 2003. "Combustion noise measurement system for low emissions combustor performance optimization and health monitoring". ASME Paper GT2003-38255.

[10] FERRARA, G., FERRARI, L., AND SONNI, G., 2005. "Experimental characterization of a remoting system for dynamic pressure sensors". ASME Paper GT2005-68733.

[11] STRAUB, D. L., FERGUSON, D. H., ROHRSSEN, R., AND PEREZ, E., 2007. "Design considerations for remote high-speed pressure measurements of dynamic combustion phenomena". AIAA Paper 2007-561.

[12] KONLE, H. J., PASCHEREIT, C. O., RÖHLE, I., AND RAUSCH, A., 2007. "Development of a novel technique of pressure pulsation measurements in turbomachinery: fiber optic microphone". AIAA Paper 2007-3444.

[13] BAKE, F., MICHEL, U., AND RÖHLE, I., 2007. "Investigation of entropy noise in aero-engine combustors". *J. Prop. Power,* **129**, pp. 370–376.

[14] MOECK, J. P., BOTHIEN, M. R., GUYOT, D., AND PASCHEREIT, C. O., 2006. "Phase-shift control of combustion instability using (combined) secondary fuel injection and acoustic forcing". In *Proc. 1st Conf. Active Flow Control*, Berlin, Germany.

[15] TIJDEMAN, H., 1975. "On the propagation of sound waves in cylindrical tubes". *J. Sound Vib.,* **39**(1), pp. 1–33.

[16] FORSTER, S., RÖHLE, I., AND MICHEL, U., 2004. Optimierung der passiven und aktiven Dämpfung von thermoakustischen Schwingungen. Final report AG Turbo II project 4.4.2.C, Deutsches Zentrum für Luft- und Raumfahrt, Berlin.

[17] PASCHEREIT, C. O., SCHUERMANS, B., POLIFKE, W., AND MATTSON, O., 2002. "Measurement of transfer matrices and source terms of premixed flames". *J. Eng. Gas Turb. Power,* **124**, pp. 239–247.

[18] PEAT, K. S., 1982. "Evaluation of four-pole parameters for ducts with flow by the finite element method". *J. Sound Vib.,* **84**(3), pp. 389–395.